Fourier filter LGS wavefront sensing for ELT size telescopes

Francisco Oyarzun, Vincent Chambouleyron, Benoît Neichel, Thierry Fusco, Andrés Guesalaga

Fourier filter LGS wavefront sensing for ELT size telescopes

Francisco Oyarzún[a], Vincent Chambouleyron[b], Benoit Neichel[b], Thierry Fusco[b], and Andrés Guesalaga[a]

[a]Departamento de Ingeniería Eléctrica, Pontificia Universidad Católica de Chile, Santiago, Chile
[b]Aix Marseille Univ, CNRS, CNES, LAM, Marseille, France

ABSTRACT

All the upcoming Extremely Large Telescopes (ELTs) include artificial Laser Guide Stars (LGS) to increase the sky coverage of their Adaptive Optics (AO) systems. Given the thickness of the sodium layer, where the LGS are created, these artificial stars end-up to be extended 3D objects. On a large pupil, like the ELTs, the sub-apertures of a Shack-Hartmann wavefront sensor see the LGS as an elongated object depending on their position with respect to the laser lunch telescope. As a result, a detector with a large number of pixels per sub-aperture is required to fully sample the elongated spots and minimize centroiding errors. As an alternative, we propose to explore the use of Fourier Filter Wavefront Sensors (FFWFS), such as the pyramid WFS but not only, as they could potentially offer an interesting alternative, significantly less pixel-intensive. As a first step, we developed a new method of simulating extended sources for FFWFS, which allows accelerating the simulation by a factor of over sixty times when compared to the traditional methods. Taking advantage of this, we then compare the performance of three sensors: the well-known Pyramid, the Ingot (as proposed by Ragazzoni) and a new promising candidate called the tilted Shearing interferometer. Sensitivity tests are performed for quantitative comparisons between these sensors. When comparing the sensitivity of a diffraction limited source with a 2D 1" source for a 3- and 4-sized Pyramid WFS, a 25 factor decrease was observed. This lost sensitivity is equivalent to a decrease in limiting magnitude of 6.7. Then, comparing the sensitivity of the Pyramid WFS and the Ingot WFS, the both had a similar behavior in the horizontal direction (across the elongation of the LGS), but the Pyramid had almost twice the sensitivity along the elongation, meaning that overall the Pyramid is more sensitive than the Ingot. The Tilted Shearing interferometer did not performed as expected, mainly because of diffraction and sampling effects that could be better understood in laboratory conditions.

Keywords: Pyramid wavefront sensor, WFS, LGS, ELT, Ingot wavefront sensor

1. INTRODUCTION

The use of laser guide stars (LGS) makes it possible to increase the coverage of adaptive optics (AO) systems, due to the lack of natural guide stars (NGS) bright enough to be able to correct atmospheric aberrations.[1] These laser stars are generated by exciting sodium atoms present in a layer of the atmosphere located approximately 90 km above sea level. Due to the width of the laser beam, the spot has a radial extension. Typical LGS' have a diameter of 1 arcsec at 90 km. Also, the sodium layer has a thickness of between 10 to 20 km, which makes the artificial star a 3D extended object.[2]

On a large pupil, like the Extremely large telescopes (ELT), the sub-apertures of a Shack-Hartmann wavefront sensor see the LGS as an elongated object depending on their position with respect to the laser launch telescope. As a result, a detector with a large number of pixels per sub-aperture is required to fully sample the elongated spots and minimize centroiding errors. At the scale of the ELTs such a detector is difficult to realize.[3]

Considering that ELTs are being designed to use SH sensors,[4] it seems appropriate to study the possibility of using other wavefront sensors for LGS wavefront sensing. Various authors have proposed the use of a pyramid

Further author information:
Francisco Oyarzun.: E-mail: ftoyarzun@uc.cl, Telephone: +569 69192506
Engineering science master's student at Pontificia Universidad Católica de Chile

wavefront sensor (Top row Fig. 1) as a replacement for the SH for ELTs, due to advantages such as adjustable sensitivity and dynamic range during operation[5] and the lower number of pixels required for the detector.[3,5] Another option for LGS wavefront sensing is the Ingot wavefront sensor[6] (Iwfs). The Iwfs takes into account the z elongation of the LGS by using a prism roof with three faces[7] (center row Fig. 1). The idea is to match the geometry of the LGS with the Iwfs such that the light is split following the elongation, optimizing the signal-to-noise ratio of the measurement.

Another idea is to build a Fourier mask that acts as a shearing interferometer. The mask is similar to the pyramid's, but instead of having four planes to generate four separated pupils, a repeating grid of planes is used to generate two pairs of pupils, the first overlapping with shear in the x-direction and the second in the y-direction (bottom row Fig. 1). The idea of the repeating grid is to make the wavefront sensor translation invariant, to retrieve some of the lost sensitivity due to the LGS' elongation. Using a spatial light modulator it would be possible to generate the mask and then tilt the whole apparatus to follow the elongation of the LGS, obtaining a similar effect as the Ingot, where the samples interact in focus with the mask.

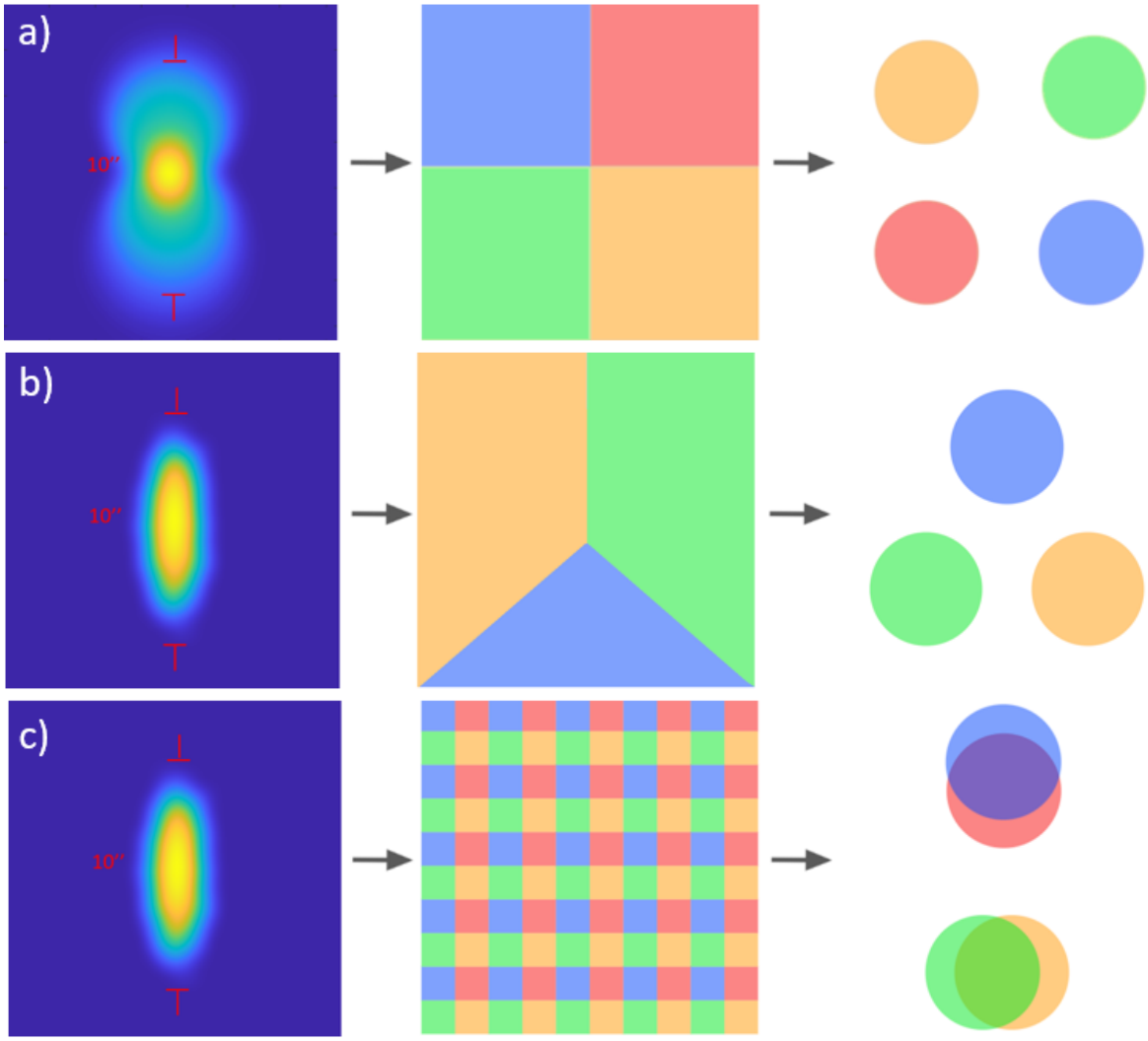

Figure 1. Diagrams of the three FFWFS tested. Top row: Pyramid WFS; central row: Ingot WFS; bottom row: titled Shearing interferometer. Left column: LGS as seen by the Fourier mask (logarithmic scale in the intensity). Note that in a) the LGS is only focused on the center, while in b) and c) the LGS is completely in focus); central column: Fourier mask, color-coded to match the pupil images with the part of the mask that generated it; right column: pupil distribution on detector plane.

The general objective of this work is to understand the behavior of different wavefront sensors in large aperture operation, such as the ELTs, in order to better comprehend the limiting factors and possible innovations in wavefront sensing.

The specific objective of this work is to measure the photon noise sensitivity to spatial frequencies, vertical and horizontal, for different wavefront sensor options for LGS wavefront sensing for the ELT, in order to determine the best suited for large aperture operation. To do this, an end-to-end simulation was developed using the Object Oriented Matlab Adaptive Optics toolbox (OOMAO).[8]

2. METHODOLOGY

2.1 LGS sampling

In order to simulate an LGS it was necessary to discretize the sodium layer into samples, and make an incoherent sum of the contribution of each one to the measurement. In a real life scenario, the laser guide star is generated by exciting tens of trillions of atoms present in the sodium layer. From a simulation point of view, that amount of samples is difficult to achieve, therefore tests were performed to identify a suitable number of samples (10.000) from which the results were not dependent on their quantity.

The sodium density profile present in the layer affects the shape, height and light distribution that comes from the LGS. Using this sodium density profile, and the geometry of the laser launch telescope, the LGS was sampled using a Monte Carlo approach.

To draw the position in the x axis coordinate of the LGS samples, a 1 arcsecond FWHM Gaussian profile centered at zero was used. For the Y coordinate, a Gaussian with the same FWHM as the X coordinate, but centered at the side of the telescope, to encode the size and position of the laser launch telescope, located at the side of the telescope pointing straight up. For the Z coordinate of the LGS samples, the sodium profile was used as the probability density function to draw the values. Examples of two sodium profiles are shown in figure 2.

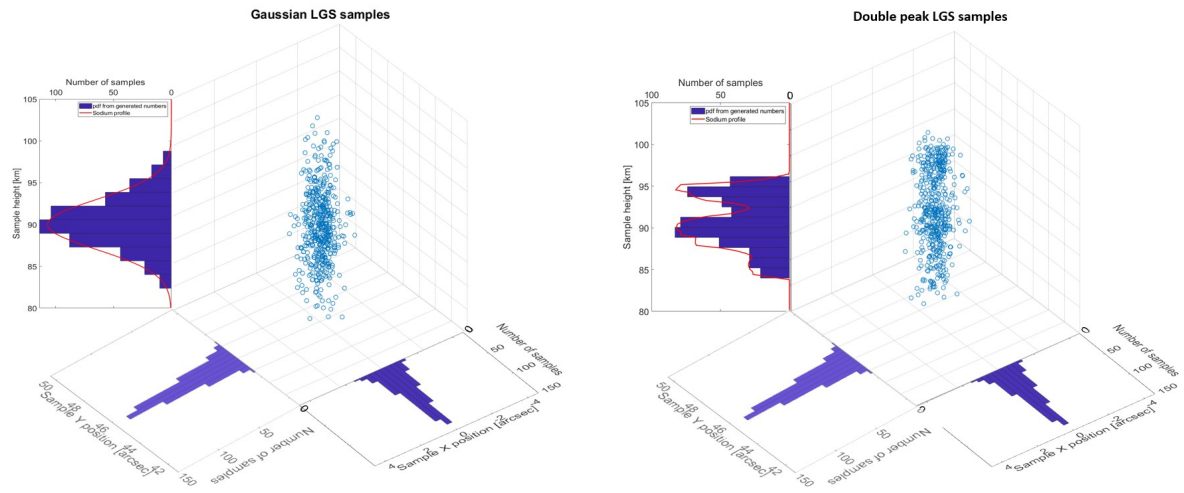

Figure 2. Sample distribution of the LGS for two sodium profiles (300 samples for better visualization). Left panel: Gaussian profile with $\mu = 90\,km$ and $FWHM = 7\,km$; right panel: double peak profile example.

2.2 Propagation

Using geometry, it is possible to calculate that the elongation of the LGS in the Y axis is approximately 10". Considering a pixel sampling of 2.4 pixels per FWHM of the PSF, a 40 m primary mirror diameter, and $\lambda = 589\,nm$, to sample the whole 10" a 10.000 x 10.000 pixel matrix would be needed. Figure 3 is an example of a pyramid wavefront sensor used with an LGS, where to fit the whole elongation of the star a 10.000 x 10.000 matrix was needed.

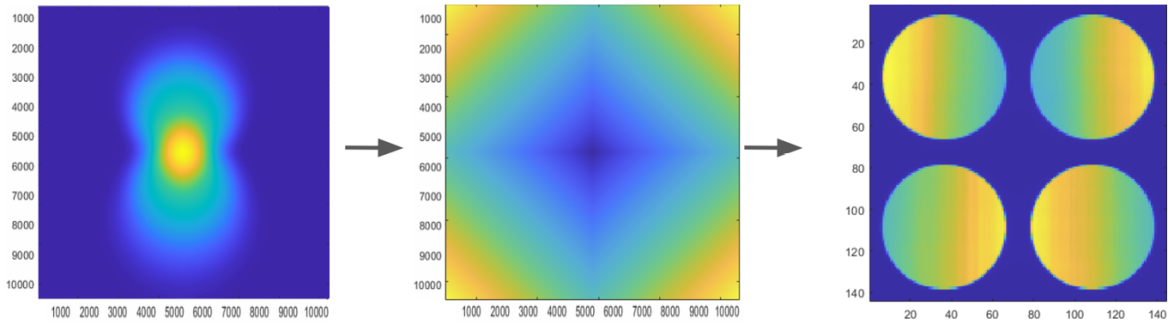

Figure 3. Representation of light path from the LGS through the pyramid and to detector (all units in pixels). Left image: log scale of the LGS spot; center image: pyramid mask; right image: pupils in the detector

Given that the telescope has to focus at a certain height ($\sim$ 90 km) each sample away will have a defocus coefficient given by it's Z coordinate. This defocus will affect the spot size as can be seen in figure 4. Even the samples with the biggest defocus coefficient only use a small number of pixels when compared to the overall elongation.

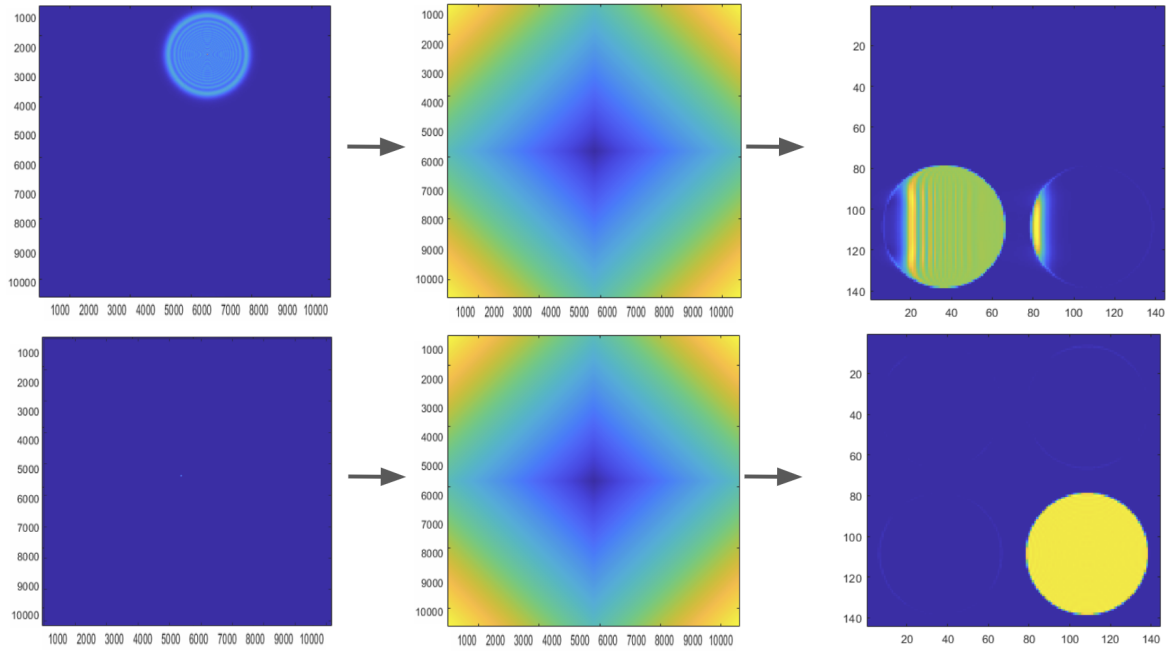

Figure 4. Representation of light path from a single sample to detector (all units in pixels). **Top row: LGS lower edge sample.** Left image: sample psf; center image: pyramid mask; right image: pupils in the detector. **Bottom row: LGS near center sample.** Left image: sample psf (as sample is near perfect focus, it looks only as a dot at the center of the image); center image: pyramid mask; right image: pupils in the detector.

Instead of adding the equivalent tip and tilt given the sample's position in the sky and using the complete LGS field of view, a more efficient way to propagate the samples is to build an appropriate sized window around the sample given by its defocus coefficient, compute the x and y position of the sample in the image plane, and translate the Fourier filter that amount. Therefore, each sample only required a small field of view and the

computation runs much faster. Figure 5 shows examples using three samples with different defocus coefficients and the simulation scaled up to match the sample's spot size.

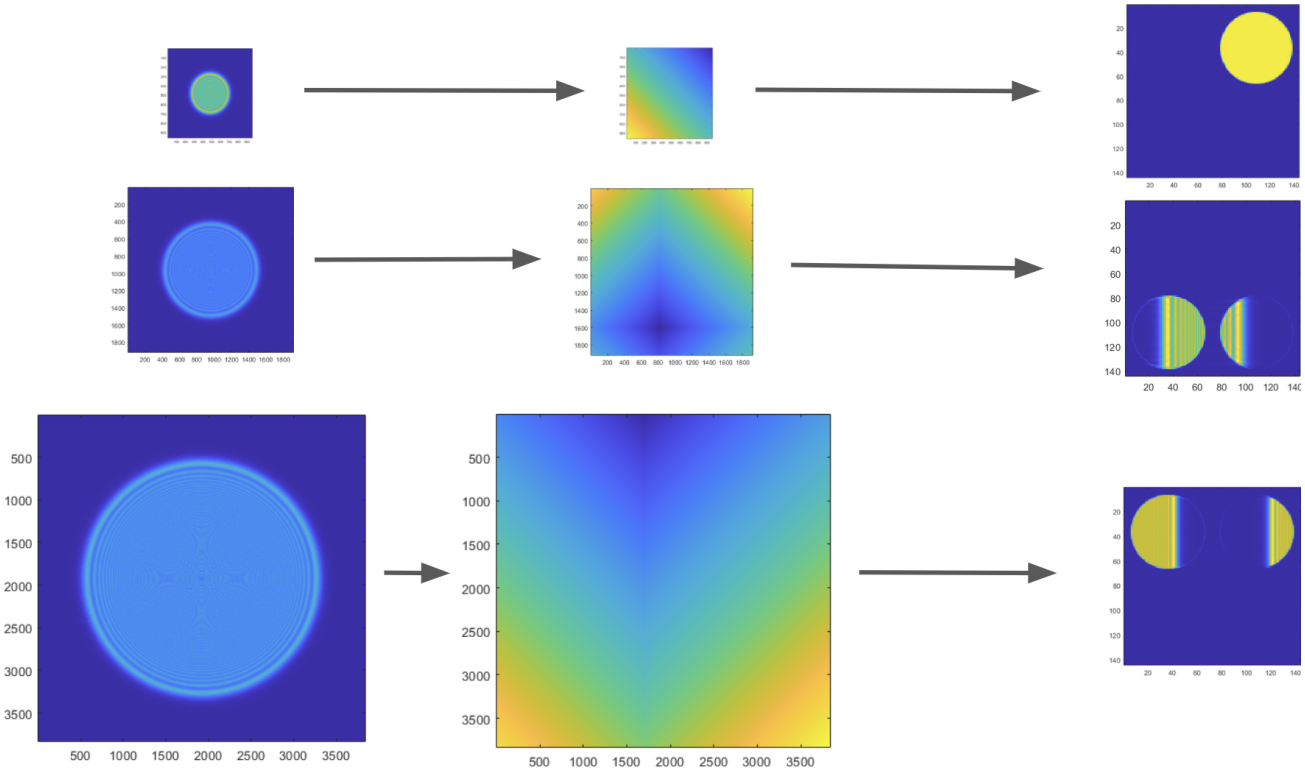

Figure 5. Light path from samples in different parts of the LGS (all labels in pixels). The telescope was focused at a height of 90 km. Top row: sample at 91 km; middle row: sample at 92 km; bottom row: sample at 96 km. left column: point source affected by defocus; middle column: portion of the pyramid the sample interacts with; right column: associated pupils' image in the detector.

This technique, that we call **portion propagation**, brings two benefits: 1) matrices are at least 10 times smaller than when using the full field of view for the LGS, and might be 50-100 times smaller for near focus samples. 2) Computation times are faster. As an example, when simulating a pyramid wavefront sensor for a 20 m telescope, the time for each frame went from 1200 to 17 seconds, so a 60 times gain in time.

2.3 Fourier filter masks as Wavefront sensors

Placing an amplitude or phase mask in an image plane can transform phase information into intensity variations.[9] These are called Fourier filter wavefront sensors. A classical example is the pyramid wavefront sensor,[10] where a glass pyramid is placed in the focal plane to separate the light into four pupils.

In order to simulate the Iwfs as a Fourier filter mask, the approach used was to eliminate the defocus coefficient from the samples, and then propagating them through a three sided pyramid (3Pyramid), aligning the elongation of the LGS with one of the edges and also shifting the 3Pyramid such that the three pupils formed had the same intensity. This approach encodes the fact that the Iwfs follows the 3D elongation of the LGS, so the mask acts on each sample in focus. Considering the full geometry of the problem, each sample would see the mask with a different perspective,[7] but having the mask not change from sample to sample could be enough to understand the expected response of the system. Figure 1, central row, shows the light path to simulate the Ingot wavefront sensor. In the figure, the LGS is shown completely in focus, given the interaction of the light with the rooftop. As all the samples are in focus, they need a small field of view for the portion propagation, making the simulation more than 200 times faster than for the Pyramid wavefront sensor. The tilted Shearing Interferometer WFS was simulated in a similar way as the Iwfs, propagating all the samples in focus through the repeating mask.

The signal and the sensitivity were obtained using the meta-intensity (using the return-to-reference operation) and its 2-norm, respectively, as presented in the work by Fauvarque et al.[9] For each of the tested WFS, a reference frame could be computed by propagating the LGS samples without atmosphere.

The sensitivity can then be used to understand the limiting magnitude of a system, as the residual phase in the error budget due to photon noise, σ^2_{noise}, depends on the sensitivity as follows[11]

$$\sigma_i^2 = \frac{1}{N_{ph} s_\gamma(i)} \tag{1}$$

$$\sigma^2_{noise} = \sum_{i=1}^{n} \sigma_i^2 \tag{2}$$

with N_{ph} the number of photons in each frame, $s_\gamma(i)$ the sensitivity to mode "i", and n modes corrected in the closed loop operation.

3. RESULTS AND DISCUSSION

Along with the computation of the sensitivities for the Pyramid, Ingot and tilted repeating Shearing interferometer wavefront sensors with LGS, some reference cases were also tested: diffraction limited source using a 3-sided pyramid and classic shearing interferometer, and laser launch telescope 1 arcsec limited source for 3- and 4-sided pyramids. The results for the photon noise sensitivity to horizontal and vertical spatial frequencies is presented in Fig 6

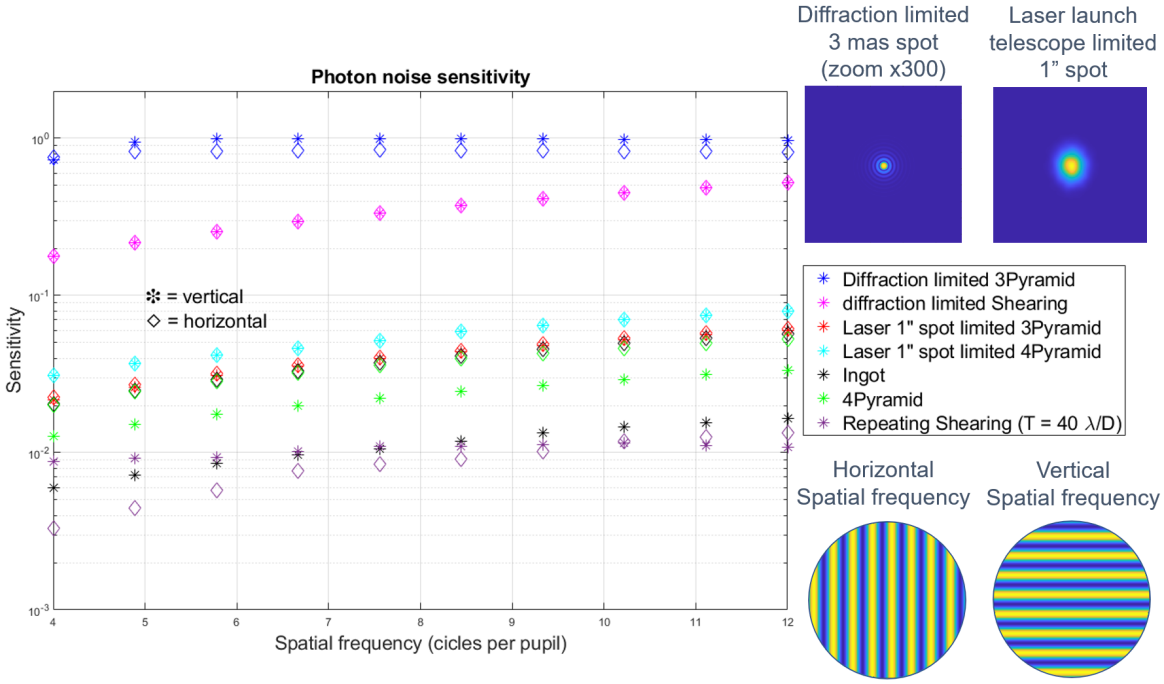

Figure 6. Photon noise sensitivity to spatial frequencies for pyramid, ingot and repeating shearing interferometer wavefront sensors. "NPyramid" refers to a N-sided pyramid. The ⋄ and ∗ makers refers to horizontal and vertical spatial frequencies, respectively.

The spatial period of the repeating shearing is 40 λ/D = 120 mas, meaning that there are 8 cycles within the FWHM of the laser spot in the "X" direction and 30 in the "Y".

From Fig 6 it is possible to observe that when going from a diffraction limited source (blue markers) to a 1" laser spot (cyan and red markers), there is a drop in sensitivity of almost 25 fold, even when there is no "Z"

elongation present, just the "XY" extension of the source. This effect probably limits the maximum sensitivity that could be obtained when using a full 3D elongated source. Using equations 1 and 2, this drop in sensitivity has the same effect in the residual variance due to photon noise as increasing the magnitude of a diffraction limited source by 6.7 magnitudes (e.g. if the limiting magnitude for the AO system using a natural star is 15, then using a 1" source the limiting magnitude would be in the order of 8-9).

When comparing the 3- and 4-sided pyramid with the laser 1" spot limited, it is possible to observe that the 4Pyramid is approximately 25 % more sensitive than the 3Pyramid. This means that the limiting sensitivity for the Pyramid and the Ingot might be different.

The 4Pyramid with the 3D elongated laser guide star shows a lower sensitivity than with the 1" spot limited source in both directions, which agrees with what is expected. The vertical sensitivity is approximately two thirds of the horizontal, which is due to the elongation being in that direction. The defocus of the samples has two effects: on one side, it lowers the sensitivity due to the light being spread out over a larger area, acting as a modulation which reduces the sensitivity, but on the other side, the size of the samples increases the dynamic range of the system, which in turn brings some of the lost sensitivity due to saturation. Samples that, if they were in focus, only would go through a single tilted plane of glass (that brings no information), now with the the defocus can interact with more than one plane, effectively raising the sensitivity.

Then, looking at the Ingot curve it is possible to observe that the horizontal frequency response is similar to the laser 1" spot of the 3Pyramid, meaning that by following the elongation with the rooftop prism this sensitivity is recovered. In contrast, the sensitivity to the vertical frequencies is greatly reduced, having a value approximately three times less than for horizontal ones. This might be explained as only a small portion of the samples "see" a filtering across the vertical direction.

When comparing the curves from the Pyramid and the Ingot is possible to observe that both have a similar sensitivity to the horizontal frequencies, even when the ingot is acting on the samples in focus. This might be explained with the fact that the limiting sensitivity of the pyramid (the 1" spot) is greater than for the Ingot, therefore, even when some sensitivity is lost due to the defocus of the samples, the overall greater sensitivity of the 4Pyramid compensates this effect. Then, when looking at the vertical sensitivities, the Pyramid has twice the sensitivity than the Ingot. In the Pyramid, not only the samples that are centered in the edge of the mask provide signal (as in the case of the Ingot), but also samples further away due to their size from the defocus.

As for the Repeating tilted shearing interferometer, it did perform as well as expected, probably because the diffractive nature of the repeating mask. As both the source and the mask are sampled using the same grid, if the period of the mask was not an integer multiple of the sampling rate of the source (pixels in the FWHM), then spillover would occur, which artificially affected the signal. Also, due to diffraction, ghost images of the pupils would appear, therefore the period of the mask could not be lowered more than 40 λ/D, because the separation of the ghost pupils would interfere with the signal. The complete separation of the pupils could be achieved if the period of the mask matched the sampling rate of the source, but probably due to aliasing the signal was unusable.

To test the sensitivity of the Tilted Shearing interferometer, an experimental approach might be a better alternative. Using a spatial light modulator (SLM), the repeating mask can be applied to an analog source of light, therefore decoupling the grid used for the mask and the source. To do this, the LOOPS optical bench[12] at LAM might be a good alternative, as there are already optical paths that go through an SLM with the purpose of doing adaptive optics. Also, another alternative would be using the new PULPOS adaptive optics bench at Pontificia Universidad Católica de Valparaiso.

The results presented above does not represent the whole performance of the tested wavefront sensors, as for example the linearity and dynamic range were not tested. The main conclusions that can be extracted from the results are

- Going from a diffraction limited source to a 1" source can lower the sensitivity of an NPyramid wavefront sensor by a factor of 25, which imposes a limit on the maximum sensitivity that can be achieved using LGS with a Pyramid-like WFS.

- The higher sensitivity of the 4Pyramid compared to the 3Pyramid for the 1" source and the increased dynamic range of the unfocused LGS can make the standard 4Pyramid a more sensitive instrument than the Ingot wavefront sensor for LGS wavefront sensing.
- The tilted Shearing interferometer might be better explored using a laboratory approach, due to diffraction and sampling effects.

4. FURTHER WORK

In the future, linearity, dynamic range and closed loop operations would provide a more general performance of the tested wavefront sensors, and also laboratory tests using the LOOPS or PULPOS bench, to better understand their behavior and to help in the decision of the best wavefront sensor to be used for LGS wavefront sensing in he new extremely large telescopes.

ACKNOWLEDGMENTS

We would like to thank SPIE, the Dirección de Postgrado de la Escuela de Ingeniería de la Pontificia Universidad Católica de Chile and the Chilean Agency for Research and Development (ANID) (grants Fondecyt 1190186 and Millennium Nucleus ACIP Science Initiative Program - NCN19_161) for their collaboration in the funding of this project. Special thanks to Jean-Francois Sauvage, Clementine Bechet, Felipe Pedreros, Camilo Weinberger, Jorge Tapia and Esther Soria for their guidance.

This work benefited from the support of the the French National Research Agency (ANR) with WOLF (ANR-18-CE31-0018), APPLY (ANR-19-CE31-0011) and LabEx FOCUS (ANR-11-LABX-0013); the Programme Investissement Avenir F-CELT (ANR-21-ESRE-0008), the Action Spécifique Haute Résolution Angulaire (ASHRA) of CNRS/INSU co-funded by CNES, the ECOS-CONYCIT France-Chile cooperation (C20E02), the ORP H2020 Framework Programme of the European Commission's (Grant number 101004719) and STIC AmSud (21-STIC-09).

REFERENCES

[1] Tyson, R. K., [*Introduction to adaptive optics*], vol. 41, SPIE press (2000).

[2] Olivier, S. S. and Max, C. E., "Laser guide star adaptive optics: present and future [invited]," in [*Very High Angular Resolution Imaging*], Robertson, J. G. and Tango, W. J., eds., **158**, 283 (Jan. 1994).

[3] Fusco, T., Neichel, B., Correia, C., Blanco, L., Costille, A., Dohlen, K., Rigaut, F., Renaud, E., Bonnefoi, A., Ke, Z., et al., "A story of errors and bias: The optimization of the lgs wfs for harmoni," in [*AO4ELT6*], (2019).

[4] Uhlendorf, K., Espeland, B., Gardhouse, R., Conan, R., and Bouchez, A., "The opto-mechanical design of the LTAO WFS for the Giant Magellan Telescope," in [*Proceedings of the Third AO4ELT Conference*], Esposito, S. and Fini, L., eds., 10 (Dec. 2013).

[5] Esposito, S., Agapito, G., Giordano, C., Puglisi, A., Pinna, E., Blain, C., and Bradley, C., "Pyramid wavefront sensing using Laser Guide Star for 8m and ELT class telescopes," in [*Adaptive Optics Systems V*], Marchetti, E., Close, L. M., and Véran, J.-P., eds., *Society of Photo-Optical Instrumentation Engineers (SPIE) Conference Series* **9909**, 99096B (July 2016).

[6] Ragazzoni, R., Portaluri, E., Viotto, V., Dima, M., Bergomi, M., Biondi, F., Farinato, J., Carolo, E., Chinellato, S., Greggio, D., et al., "Ingot laser guide stars wavefront sensing," *arXiv preprint arXiv:1808.03685* (2018).

[7] Di Filippo, S., Greggio, D., Bergomi, M., Radhakrishnan, K., Portaluri, E., Viotto, V., Arcidiacono, C., Magrin, D., Marafatto, L., Dima, M., et al., "Ingot wavefront sensor: from the optical design to a preliminary laboratory test," *arXiv preprint arXiv:2101.07742* (2021).

[8] Conan, R. and Correia, C., "Object-oriented matlab adaptive optics toolbox," in [*Adaptive optics systems IV*], **9148**, 91486C, International Society for Optics and Photonics (2014).

[9] Fauvarque, O., Neichel, B., Fusco, T., Sauvage, J.-F., and Girault, O., "General formalism for fourier-based wave front sensing," *Optica* **3**(12), 1440–1452 (2016).

[10] Ragazzoni, R., "Pupil plane wavefront sensing with an oscillating prism," *Journal of modern optics* **43**(2), 289–293 (1996).

[11] Chambouleyron, V., *Optimisation de l'analyse de surface d'onde par filtrage de Fourier pour les systèmes d'optique adaptative à hautes performances*, PhD thesis, Aix-Marseille university (2021).

[12] Janin-Potiron, P., Chambouleyron, V., Schatz, L., Fauvarque, O., Bond, C. Z., Abautret, Y., Muslimov, E. R., El Hadi, K., Sauvage, J.-F., Dohlen, K., et al., "Adaptive optics with programmable fourier-based wavefront sensors: a spatial light modulator approach to the lam/onera on-sky pyramid sensor testbed," *Journal of Astronomical Telescopes, Instruments, and Systems* **5**(3), 039001 (2019).